NASA TECHNICAL MEMORANDUM

NASA TM X-67862

NASA TM X-67862

AN INVESTIGATION OF GAS DYNAMIC AND TRANSPORT PHENOMENA IN THE TWO-DIMENSIONAL JET INTERACTION FLOWFIELD

by W. J. Thayer, III and R. C. Corlett
Lewis Research Center
Cleveland, Ohio

TECHNICAL PAPER proposed for presentation at Fourth Fluid and Plasma Dynamics Conference sponsored by the American Institute of Aeronautics and Astronautics
Palo Alto, California, June 21-23, 1971

AN INVESTIGATION OF GAS DYNAMIC AND TRANSPORT PHENOMENA IN THE TWO-DIMENSIONAL JET INTERACTION FLOWFIELD*

by W. J. Thayer, III**

U.S. Army Air Mobility R&D Laboratory
National Aeronautics and Space Administration
Lewis Research Center
Cleveland, Ohio

and

R. C. Corlett

University of Washington
Seattle, Washington

Abstract

Pressure, temperature, gas sampling, and optical measurements were made in the turbulent separated flow region upstream of jets. Hot hydrogen, helium, and nitrogen were injected from a converging slot nozzle perpendicular to the heated Mach 2.5 airstream above a flat plate. The dependence of the separation distance, wall pressure, and side force on the jet to free stream pressure and density ratios and the separation Reynolds number was determined. The recirculation region injectant concentration was high. An experimental technique employing tracer gas injection was proposed and implemented to determine air and injectant mass transport rates through the separated flow region.

Nomenclature

A_c amplification factor

c sonic velocity

d slot width

F force or thrust

h height of jet or step

ℓ distance from leading edge of model

---

*This work was supported by the Boeing Scientific Research Laboratories.

**Formerly Basic Research Associate, Boeing Scientific Research Laboratories, Seattle, Washington.

L	distance from leading edge to slot nozzle
M	Mach number
m	mass
$\dot{m}$	mass flow rate
P	nondimensionalized flowfield property
p	pressure
Re_ℓ	Reynolds number based on length, $Re_\ell = \frac{\rho_f u_f \ell}{\mu_f}$
Re_x/x	unit Reynolds number $= \frac{\rho_f U_f}{\mu_f}$
s	jet or step span
T	absolute temperature, ^oR
u	velocity parallel to the plate
V	volume
$\dot{V}$	volume flow rate
W	mass flux ratio
w	mass flux
X_i	mole fraction of species i
x	axial distance, from slot nozzle or stepface, positive upstream
Y_i	mass fraction of species i
α	boundary layer separation angle
γ	specific heat ratio
μ	absolute viscosity
ρ	density
τ	time

Subscripts:

a	property of the wind tunnel airstream at $M = 2.5$
ar	air passing through the upstream recirculation region
e	property of jet nozzle exit
f	free stream condition
j	jet
jr	injectant passing through the upstream recirculation region
jv	related to a jet exhausting into a vacuum
oa	air stagnation condition
oj	jet stagnation condition
p	plateau
r	residence time
rec	upstream recirculation region
s	jet normal shock, or computed nozzle width
sep	separation
ss	start of the separation pressure rise
t	tracer gas
to	component t at time zero
1.5	location at which $p/p_f = 1.5$

I. Introduction

Injection of secondary jets into a supersonic stream is of interest for thrust vector control, hypersonic vehicle control, and supersonic combustion applications. Several distinctly different injector geometries have been previously investigated for each application. This work deals with the interaction of a highly underexpanded jet with a Mach 2.5 airstream. The converging slot nozzle used in this series of experiments was oriented perpendicular to the primary stream. This gas injection process is referred to as "transverse injection," and the resulting flow as the "jet interaction flowfield." Transverse injection causes separation of the boundary layer upstream of the jet, as depicted in Figure 1(a). The wall pressure distribution characteristic of the turbulent flow studied, and some associated terminology, are shown in Figure 1(b). Properties of the separated flow region which may be important in supersonic combustion applications of transverse gas injection were investigated.

Transverse injection from slot nozzles has been studied extensively during the past decade.[1-4] Although the slot nozzle has possible applications in chemically reacting flows, most previous work has been directed at determining the wall pressure distribution and flow geometry for jet interaction control applications. As a result, neither heat nor mass transfer data are available for the separated flow region upstream of a jet. Since most previous investigations have been conducted with ambient temperature air and injectant streams, the dependence of the interaction flow geometry and pressure field on several important parameters is not definitely known. Therefore, flowfield properties of importance in the spontaneous ignition and combustion of chemically reactive injectants, and those of interest in jet interaction control applications, were investigated. These properties include the chemical composition, temperature, and mass transport rates of injectant and air, as well as the frequently measured wall pressure distribution. The objective of this work was to determine the dependence of these flow properties on the parameters which control the flowfield. Several of these parameters were separately varied to determine the dependence on each. A unique capability to independently vary the airstream temperature and pressure, the injectant temperature and pressure, and the species injected made this possible. A "well mixed" model of the separated flow region is proposed and used with the flow measurements to determine the mass transport rates in this region. This work suggests that the separated flow region will control spontaneous ignition at sufficiently high temperature, as was observed in a subsequent phase of this work. The chemically reacting flow was investigated and the results of this investigation were reported in Ref. 5.

II. A "Well Mixed" Model of the Separated Flow Region

A novel, experimental technique was used in this investigation to estimate the mass transport rates of air, $\dot{m}_{ar}$, and injectant, $\dot{m}_{jr}$, into and out of the recirculation region upstream of a transverse jet. The basis of this technique is the assumption that the recirculation region is "well mixed," a term which will be defined below. This assumption makes possible the evaluation of the ratio of the air and injectant transport rates, $\dot{m}_{ar}/\dot{m}_{jr}$, from the composition of the region. A second assumption makes possible an approximate experimental determination of the magnitudes of $\dot{m}_{ar}$, $\dot{m}_{jr}$, and of residence time of the mixture within the recirculation region, τ_r.

Gas particles that enter the separated flow region circulate within this region for some time before turbulent transport sweeps them out and replaces them. Air enters the recirculation region through the separated boundary layer by a turbulent mixing process, Figure 2. Injectant enters the region through the jet shear layer by a similar process. A mixture of injectant and air of equal mass simultaneously leaves the region through these mixing layers. Because gas is swept around the recirculation region for some time before it leaves, it has an excellent opportunity to mix with gas already in the region. It was assumed that when air and injectant enter the recirculation region, these gases mix with the gas already in the region in a period of time short compared with the time that the gases remain in the region. A recirculation region exhibiting this behavior is called "well mixed" in the remainder of this discussion. An extremely well mixed condition corresponds to instantaneous mixing of gas entering the region with gas already in the region, and a homogeneous mixture within the region. This concept is very similar to that proposed by Longwell et al.[6] for recirculation zones downstream of bluff body flameholders, and later used to develop the "perfectly stirred reactor" for making overall reaction rate measurements.[7] Since the flow is steady in the mean, the mixture in the recirculation region reflects the relative transport rates of injectant and air through the region. The mass fraction of injectant in this well mixed region is proportional to the mass flow rates of injectant and air through the region, i.e.

$$Y_{inj} = \frac{\dot{m}_{jr}}{\dot{m}_{jr} + \dot{m}_{ar}}$$

Or, upon rearranging this expression

$$\frac{m_{ar}}{m_{jr}} = \left(\frac{1}{Y_{inj}} - 1\right) \quad (1)$$

Thus, gas samples taken from a well mixed recirculation region can be used to calculate the ratio of $\dot{m}_{ar}$ and $\dot{m}_{jr}$. However, some independent means must be used to evaluate either $\dot{m}_{ar}$ or $\dot{m}_{jr}$ before this result can be used to determine the magnitude of the other mass flow rate.

The possibility of determining either transport rate by analyzing the complicated upstream recirculation region seemed remote when this investigation began. Therefore, an independent experiment was planned to quantify the mass transport rates. The technique chosen consisted of bleeding tracer gas into a well mixed recirculation at a known rate, taking gas samples to determine the mass fraction of tracer in the region, and using Eq. (1) to evaluate the ratio of the mass transport rate to the known tracer gas transport rate. If tracer gas could be injected uniformly across region upstream of a jet, Eq. (1) would take the form

$$\frac{\dot{m}_{ar} + \dot{m}_{jr}}{\dot{m}_{tr}} = \left(\frac{1}{Y_{tr}} - 1\right)$$

This relation and Eq. (1) could be solved simultaneously for $\dot{m}_{jr}$ and $\dot{m}_{ar}$. However, the small size and complexity of the wind tunnel model used in this experiment prohibited uniform tracer gas injection upstream of the jet.

The physical similarity between flow separation phenomena and the separated flow regions upstream of transverse jets and forward facing steps has been frequently discussed in the literature,[3,8] and suggested another approach for determining the transport rates. An assumption, based on this similarity, made possible an experimental technique for estimating $\dot{m}_{ar}$. It was assumed that the average mass flux of air, w_{ar}, transported across the separated turbulent boundary layer upstream of a jet is equal to the transport mass flux upstream of a forward facing step which results in the same geometry separated flow region at identical free stream conditions. Thus, if the lengths of the separated boundary layers are equal, and the free stream conditions are identical, the mass transport rates of air across the boundary layers are equal, i.e.,

$$\dot{m}_{ar_{Jet}}(T_f, p_f, x_{ss}) = \dot{m}_{jr_{FFS}}(T_f, p_f, x_{ss}) \tag{2}$$

The dependence of the air mass flux transported across the separated boundary layer upstream of a step (see Fig. 2) can be evaluated by metering tracer gas into the well mixed recirculation region and sampling the resulting mixture. Equation (1) takes the form

$$\frac{\dot{m}_{ar}}{\dot{m}_{tr}} = \frac{1}{Y_{tr}} - 1 \tag{3}$$

for this recirculating flow. Since $\dot{m}_{tr}$ and Y_{tr} can be measured through a wide range of conditions, the dependence of $\dot{m}_{ar}$ on the free stream parameters and separated flow region size may be evaluated. The average mass flux of air transported across the mixing layer may be calculated if the separated flow geometry is measured. The width of the mixing layer is equal to the step span, s, and since the separation angle is small, the length is approximately the distance from the jet or step to the start of the separation pressure rise, x_{ss} (see Fig. 1). The average mass flux, w_{ar}, is then

$$w_{ar} = \frac{\dot{m}_{ar}}{x_{ss} s} \tag{4}$$

It is convenient to nondimensionalize this mass flux by dividing by the free stream mass flux, $\rho_f u_f$, giving

$$\bar{W}_{ar} = \frac{w_{ar}}{\rho_f u_f} = \frac{\dot{m}_{ar}}{x_{ss} s \rho_f u_f} \tag{5}$$

The dependence of this dimensionless mass flux on the free stream conditions may be determined using the tracer gas injection technique to evaluate the air mass transport rate. Once this dependence has been determined, the result can be used to evaluate the injectant mass transport rate through the recirculation region upstream of a jet. Using Eq. (5) to evaluate the air mass flow rate in Eq. (1), the injectant mass flow rate is

$$\dot{m}_{jr}(T_f, p_f, x_{ss}) = \frac{W_{ar}(T_f, p_f, x_{ss}) x_{ss} s \rho_f u_f}{\left(\frac{1}{Y_{inj}} - 1\right)} \tag{6}$$

Since each quantity may be evaluated experimentally, it is possible to estimate the transport rates through the recirculation region upstream of a transverse jet.

The time that a fluid particle remains in the recirculation region after being transported into it will be called its residence time, τ_r. The residence time is important in making estimates of ignition limits, and may be estimated once W_{ar} and $\dot{m}_{jr}$ have been evaluated. A method for doing this is developed below.

Consider again the well mixed recirculation region upstream of a jet, Fig. 3(b). This region contains a mass of fluid, m_{rec}, composed of air and injectant. The mass fraction of injectant is Y_{inj}. Air and injectant flow through this region at a net rate of $\dot{m}_{rec}$. The flow is steady, and Y_{inj}, $\dot{m}_{rec}$, and m_{rec} are constant. The process of interest is not steady, but time dependent. If a particle of fluid of mass m_{to} enters the region, it is instantaneously mixed into the entire region. The residence time is representative of the time required for the steady flow of gas through the region to flush this mass from the region. The mass, m_{to}, is not a separate species, but simply a discrete portion of the steady flow of injectant and air which has been identified for consideration. Since the system is well mixed, at time $\tau = 0$, when m_{to} entered the region, the concentration of t in the region is

$$Y_{to} = \frac{m_{to}}{m_{to} + m_a + m_{inj}} = \frac{m_{to}}{m_{rec}}$$

This concentration decreases with time as fluid enters the region, mixes, and flows out of the region containing t in the same concentration as the well mixed region at that time,

$$Y_t(\tau) = \frac{m_t(\tau)}{m_t(\tau) + m_a + m_{inj}} = \frac{m_t(\tau)}{m_{rec}}$$

The mass of fluid leaving the region is equal to the mass flow rate entering, $\dot{m}_{rec}$, but contains species t in the mass fraction $Y_t(\tau)$. Then, for the recirculation region,

$$\frac{dm_t(\tau)}{d\tau} = -\dot{m}_{rec}Y_t(\tau) = -\dot{m}_{rec}\frac{m_t(\tau)}{m_{rec}}$$

$$\frac{dm_t}{m_t} = -\frac{\dot{m}_{rec}}{m_{rec}}\,d\tau$$

$$\frac{m_t}{m_{to}} = e^{-\dot{m}_{rec}/m_{rec}\ \tau} \tag{7}$$

The residence time, τ_r, will be defined as that length of time required for the mass of t in the recirculation region to reach one percent of its initial mass, i.e.,

$$\frac{m_t(\tau_r)}{m_{to}} = 0.01 = e^{-\dot{m}_{rec}\tau_r/m_{rec}} \tag{8}$$

which implies that

$$\tau_r = 4.6\,\frac{m_{rec}}{\dot{m}_{rec}}$$

The discussion above is applicable to any well mixed recirculation region.

Transport through the recirculation region must be considered to evaluate τ_r. The turbulent boundary layer separates from the wall at an approximately constant angle, α, of 12°. The recirculation region is approximately a wedge in shape, with a length of x_{ss}, height of $x_{ss}\tan\alpha$, and a width equal to the span, s. The volume of the recirculation region is thus approximately

$$V_{rec} = \frac{s x_{ss}^2 \tan\alpha}{2}$$

The mass of gas contained in this region is

$$m_{rec} = \frac{\rho_{rec} s x_{ss}^2 \tan\alpha}{2}$$

where ρ_{rec} is the average recirculation region density. The mass flow rate through the recirculation, $\dot{m}_{rec}$, is equal to the sum of the air and injectant flow rates. The injectant mass flow rate is small when compared with the air mass flow rate, and in this approximate treatment, is neglected. The mass flow rate through the recirculation region is then, from Eq. (5)

$$\dot{m}_{rec} \doteq \dot{m}_{ar} = W_{ar} x_{ss} s \rho_f u_f$$

Using $\dot{m}_{rec}$ and m_{rec} in the relation for τ_r, one finds that

$$\tau_r = \frac{4.6\ \rho_{rec} x_{ss} \tan \alpha}{2 W_{ar} \rho_f u_f} \tag{9}$$

Thus, residence times can be estimated from the steady flow measurements.

III. Experimental Apparatus and Measurement Techniques

This investigation was carried out in the Mach 2.5 supersonic combustion wind tunnel at the Boeing Scientific Research Laboratories.[9] This wind tunnel is a blowdown facility. Air is supplied from compressed air bottles and heated in an alumina pebble bed storage heater. The air stagnation temperature is variable from ambient to 2550° R. The stagnation pressure is variable from 39 to 96 psia. The maximum constant temperature and pressure wind tunnel run duration varies from approximately three minutes for low temperature or high pressure runs to ten minutes for high temperature, low pressure runs. The air total temperature was measured with a double platinum shielded, aspirated, platinum-platinum 13% rhodium thermocouple located in the wind tunnel settling chamber. The wind tunnel stagnation pressure was displayed on a 15 inch diameter Heise gage and recorded photographically.

The experimental apparatus is sketched in Fig. 3. The flat plate wind tunnel model was built in sections to allow the use of interchangeable water cooled and uncooled parts. The flat surface of the wind tunnel model was located 1/2" above the tunnel centerline. The model spanned the 4" dimension of the 4" by 6" test section. The 0.0080 inch wide slot nozzle spanned the center 2.00 inches of the model, 5.00 inches from the leading edge. The nozzle was oriented perpendicular to the external stream. Side plates enclosed the 2.00 inch wide interaction region and extended to a location 7.00 inches downstream of the nozzle. Three-dimensional roughness elements were used to trip the boundary layer. At the separation point, the boundary layer was always turbulent and approximately 0.10 inch thick as determined from shadowgraphs. Arrays of static pressure taps were located upstream and downstream of the slot nozzle. Static pressures were displayed on a fifty tube manometer board and recorded photographically. Five chromel-alumel thermocouples were spot welded to the underside of the thin, uncooled flat plate upstream of the nozzle. Signals from these thermocouples were recorded on a Visicorder oscillograph.

A hydrogen and inert gas heater was designed and built for these gas injection experiments. A single welded joint connected the heater to the gas inlet of the wind tunnel model. The temperature of nitrogen, helium, or hydrogen could be raised from ambient up to 2450° R at pressures from 20 to 270 psia. The injectant temperature was measured with a 0.010 inch diameter chromel-alumel thermocouple located in the high velocity outlet of the heater. Direct current power was supplied by the series connection of three Miller rectifiers and one G.E. Arc Furnace Rectifier.

The injectant gases were carried to the model using a remotely operated gas control and metering system which was built for this experiment. Nitrogen, helium, and hydrogen were supplied by 40 000 standard cubic foot compressed gas trailers located outside the laboratory. Two parallel, high capacity manifold regulators were used to control the nitrogen and hydrogen or helium injection pressures. Nitrogen was used as an injectant during many runs and as the hydrogen line purge during all runs. Gas volume flow rates were measured to within one percent of the total volume flow rate using Potter and Flow Technology turbine flowmeters. The unheated injectant temperature was measured 1.5 ft upstream of the flowmeter with a chromel-alumel thermocouple. The gas pressure was measured at a tap on the flowmeter and was displayed on a 15 inch diameter Heise gage. The hydrogen and nitrogen used in this experiment were at least 99.89 and 99.95% pure, respectively.

Gas samples were drawn from the static pressure taps located in the upstream recirculation region. These samples were pumped into sample storage bottles using a remotely operated gas sampling system. Eight gas samples were taken from three static pressure taps during each run, and analyzed in a gas chromatograph between wind tunnel runs. Samples were usually taken from unmodified static pressure taps, but small probes were bonded into the taps during several runs.

With the exception of the wind tunnel total pressure, injectant pressure at the flowmeter, and static pressures, all data were recorded continuously during each wind tunnel run. The wind tunnel pressure, injectant flowmeter pressure, and plate static pressures were recorded photographically at times of interest during each run. Event markers were used to mark the continuous records when data photographs were taken. With the exception of the gas sampling measurements, all data were read, recorded, and keypunched after the wind tunnel runs. These cards were then input into a data reduction computer program for evaluation of the side force, separation distance, and other quantities of interest, and for plotting of the wall pressure distributions.

Shadowgraph pictures, using Polaroid high contrast film, were taken of the jet interaction region with and without transparent sideplates. These were taken only for the investigation of cold gas injection into ambient total temperature air. The jet normal shock height and the separation shock wave location and angle were scaled from these photographs.

The wind tunnel model, hydrogen heater, and the instruments and methods used to record data during wind tunnel runs, and the techniques for data reduction are discussed in detail in Ref. 10.

IV. Experimental Results

The results of this experimental investigation are organized into two categories for discussion in this paper; results related to flow geometry and pressure, and those related to mass transport. Although all flowfield properties depend upon the same independent parameters and were investigated simultaneously, the gas dynamic and transport results are discussed most easily as separate subjects.

This investigation was conducted after making a dimensional analysis of the flowfield. These considerations showed that an appropriately nondimensionalized flowfield property, P, depends on the following set of dimensionless groups:[10]

$$P = f\left(Re_L, M_f, \gamma_f, M_j, \gamma_j, \frac{p_{oj}}{p_f}, \frac{R_j T_{oj}}{R_f T_f}, \frac{d_j}{L}\right) \quad (10)$$

The fixed geometry of the wind tunnel and model assured that the free stream and jet Mach numbers, M_f and M_j, and the ratio d_j/L remained constant. The unique ability to independently vary both the injectant temperature and pressure and the free stream temperature and pressure, using nitrogen, helium, and hydrogen as injectants, made possible determination of the dependence of flowfield properties on Re_L, p_{oj}/p_f, $R_j T_{oj}/R_f T_f$, γ_f and γ_j. These dimensionless groups were varied independently by appropriate manipulation of the independent parameters. The results of this investigation follow.

Gas Dynamic Phenomena

The distance upstream of the slot nozzle at which separation occurs, subsequently referred to as the separation distance, and the plateau pressure level within the separated flow region were chosen as the properties which best characterize the jet interaction flowfield. The dependence of these two flow properties on the parameters which control the flowfield was extensively investigated. In addition, the amplification factor was evaluated at all conditions and its dependence on the controlling parameters is discussed in this section.

Effects of Pressure Ratio Variation

The dependence of the jet interaction flowfield on the ratio of the jet stagnation pressure to the free stream static pressure, p_{oj}/p_f, has occupied at least part of the attention of most previous investigators.[1,3,4] Previous investigations have generally utilized ambient temperature air and injectant gases. The earlier investigations exhibit rough agreement in results related to pressure ratio variation. The dependence of side force, amplification factor, and separation distance on p_{oj}/p_f found during the ambient temperature part of this investigation agrees well with previous experiments,[3,11] as was discussed in Ref. 12. The variable temperature experiments reported here demonstrate that the separation distance and amplification factor have the same functional dependence on p_{oj}/p_f throughout the range of conditions of this investigation. The separation distance dependence on the pressure ratio is readily seen in Fig. 4, in which nitrogen, helium, and hydrogen injection data are compared at identical free stream and injectant conditions. Since no simple, accurate method of determining the separation point is available, the distance upstream of the jet at which the plate pressure had increased to 1.5 times the free stream pressure, $x_{1.5}$ was used to represent the separation distance. As discussed in Ref. 10, this location is very near the separation point. The separation distance dependence on p_{oj}/p_f is correlated by the relation

$$\frac{x_{1.5}}{d_s} = a\left(\frac{p_{oj}}{p_f}\right)^{0.77}$$

The coefficient, a, depends on the injectant and free stream densities and the free stream Reynolds number. The power law dependence was anticipated, in view of previous observations indicating that the separation distance is related to the jet shock height,[1,11] and that a similar relation describes the shock height of a jet expanding into quiescent surroundings.[13] The upstream wall pressure distribution was integrated over the interaction area to evaluate the interaction force, F_i (see Ref. 10 for a detailed discussion of the data reduction procedures). The amplification factor, A_c, was computed from the measured interaction force and injectant mass flow rate, m_j, using the relation

$$A_c = \frac{F_i + F_j}{F_{jv}} = \frac{F_i + m_j c_e + A_e(p_e - p_f)}{m_j c_e + A_e p_e}$$

where F_j and F_{jv} are the thrusts of sonic jets exhausting to the free stream static pressure and into a vacuum, respectively. The sonic velocity, c_e, and the exit pressure, p_e, were calculated at the nozzle exit assuming isentropic flow. Throughout the range of temperatures, pressures, and injectants investigated, the dependence of the amplification factor on p_{oj}/p_f remained essentially identical to that determined in the cold flow experiments reported earlier, Ref. 12. The amplification factor data are correlated by the relation

$$A_c = b - 0.2 \ln \frac{p_{cj}}{p_f}$$

The coefficient, b, depends on the ratio, R_jT_{oj}/R_aT_a, in a manner which is discussed in the next section. The amplification factor, and hence the coefficient, b, does not depend on the free stream Reynolds number in the turbulent regime of this investigation. This dependence of A_c on the pressure ratio is almost identical to that reported by Werle et al.[11] for injection of air into a Mach 4 airstream.

Effects of Density Variation

The ratio of the jet and free stream densities, ρ_{oj}/ρ_f, was varied independently of the other dimensionless groups in Eq. (10). This was accomplished by changing either the injectant temperature or the species injected, with all other parameters held constant. Experiments of this type were conducted at several free stream conditions. Since the pressure ratio was held constant, a density ratio change may be represented as a variation in the ratio, R_jT_{oj}/R_aT_a. This dimensionless group is used in the presentation of data instead of the density ratio because the results showed that density variation due to pressure changes had a distinctly different effect on the flow than did changes in temperature and molecular weight. Helium was usually injected during the variable R_jT_{oj}/R_aT_a experiments to eliminate effects resulting from injectant specific heat ratio changes. Nitrogen and hydrogen were injected at several conditions to increase the R_jT_{oj}/R_aT_a range.

The separation distance increases with R_jT_{oj}/R_aT_a when low density gas is injected, as may be seen in Fig. 5, while the plateau pressure remains unchanged. The systematic variation in separation distance and amplification factor with molecular weight reported earlier by the author[13] results from a change in this parameter. This density dependence is not observed when high molecular weight, low temperature gases are injected. Two distinct regimes of dependence on R_jT_{oj}/R_aT_a are evident, as seen in Fig. 6. The separation distance, side force, and amplification factor are almost independent of molecular weight and temperature when R_jT_{oj}/R_aT_a is less than approximately 7. This result has previously been observed by Spaid,[14] Spaid and Zukoski,[3] and Allan[15] in ambient temperature experiments utilizing several high molecular weight injectants. However, these investigators did not operate in the high R_jT_{oj}/R_aT_a regime, and did not observe its existence. Each of these investigators found that helium exhibited a peculiar behavior; both the separation distance and side force were greater than those found with higher molecular weight injectants. On the basis of a semi-empirical analysis, Spaid and Zukoski[3] concluded that this increase was an effect of the injectant specific heat ratio, γ_j. Allan[15] demonstrated that γ_j variation does not affect the jet interaction flowfield, and concluded that a molecular weight effect was responsible for the increase. A variable temperature experiment has not previously been conducted in the high R_jT_{oj}/R_aT_a regime. Allan refers to unpublished data from a slot injection experiment employing air as the injectant. These experiments showed no change in side force when high temperature air was injected. This is not surprising, however, since the data of this experiment indicate that air must be heated to approximately 2200° R before a separation distance increase is noticeable. This was not possible in the experiment referred to by Allan.[15] Hydrogen has not previously been investigated in a slot injection experiment, presumably due to the hazards involved. Fig. 6 and similar data obtained at other conditions demonstrate that as R_jT_{oj}/R_aT_a increases above approximately 7, the separation distance rapidly increases. The only previous observations in this regime are the isolated data points for cold helium injection.[3,15] These results are in agreement with the behavior observed in this experiment. Associated with the separation distance increase is a similar increase in amplification factor, as seen in Fig. 7. Again, two distinct regimes seem to be present. On the basis of these results, it is concluded that, in addition to the high density regime in which the flowfield is independent of R_jT_{oj}/R_aT_a, a second regime exists in which the separation distance and amplification factor depend strongly on temperature and the injectant molecular weight.

Spark shadowgraphs were taken of the interaction region in an effort to determine the mechanism of the separation distance dependence on R_jT_{oj}/R_aT_a. Since plexiglass sideplates were used during these runs, shadowgraphs were made only of ambient total temperature flows. A comparative study of hydrogen and nitrogen injection was made. The average distance measured from the jet to the intersection of the extrapolated separation shock with the plate agrees well with the location of the separation pressure rise determined from the wall pressure data. The shadowgraphs verify the separation distance increase seen in the wall pressure data. The separation shock wave angle does not depend on the gas injected. The jet normal shock heights of equal pressure ratio hydrogen and nitrogen jets are almost identical. The separation distance increase with R_jT_{oj}/R_aT_a is definitely not due to an increase in the jet normal shock height. The only substantial differences between shadowgraphs of the hydrogen and nitrogen injection flowfields are in the region immediately above the jet normal shock and downstream of the jet. This region is always significantly larger when hydrogen is injected. As a result, the separated boundary layer appears to pass over the jet further from the plate when hydrogen is injected.

Proposing a mechanism which explains the separation distance and side force dependence on R_jT_{oj}/R_aT_a is difficult. This phenomenon is not predicted by existing semi-empirical theories.[3,8] The complexity of the interaction region makes a rigorous analysis appear unfeasible at the present time. The increase in the size of the separated flow region may result from a displacement of the external stream due to the increased volume flow rate of injectant into the recirculation region when low density gas is injected. This phenomenon may also be due to an increased effective jet height associated with the subsonic region above the jet normal shock. This phenomenon is not understood at present.

Effects of Reynolds Number Variation

The free stream unit Reynolds number was varied independently of the other dimensionless groups in Eq. (10) during this phase of the investigation. This was accomplished by changing the free stream temperature. The injectant temperature was adjusted so that the ratio R_jT_{oj}/R_aT_a was held constant. p_{oj}/p_f was maintained at approximately 85. Helium was usually injected to assure that changes in the injectant specific heat ratio would not complicate interpretation of results. Nitrogen was also injected at all conditions throughout the Reynolds number range investigated.

Both the separation distance and the plateau pressure change with the Reynolds number, as seen in Fig. 8. As the free stream Reynolds number increases, the plateau pressure decreases. Significantly, the plateau pressure is not affected by the gas injected. Data, like that in Fig. 8, taken with hydrogen, helium, and nitrogen at the same pressure ratio and unit Reynolds number, but at many values of R_jT_{oj}/R_aT_a, show identical plateau pressures. Indeed, data taken at conditions resulting in rapid combustion of hydrogen in the region upstream of the jet demonstrate that the plateau pressure is, in addition, not affected by rapid chemical heat release.[5] In addition to changing with the free stream Reynolds number, the plateau pressure was found to change slightly with any parametric variation which resulted in a separation distance change. When correlated with the Reynolds number based on the distance from the leading edge to the separation point, $Re_{\ell sep}$, all of the plateau pressure data fall on very nearly the same curve. This curve is seen in Fig. 9, and shows a plateau pressure dependence on the separation Reynolds number which is almost identical to that found by Chapman et al.[16] upstream of forward facing steps. Plateau pressure data obtained upstream of forward facing steps during the mass transport experiments of this investigation are plotted in Fig. 9. The constant plateau pressure found by Love[17] for fully turbulent boundary layer separation upstream of forward facing steps at Mach 2.5, and the point reported by Hahn[18] at Mach 2.5, are plotted for comparison. Plateau pressures at Mach 2.5 were interpolated between the data of Chapman et al.[16] at Mach 2.4 and 2.7 for turbulent boundary layer separation upstream of forward facing steps, and also correlated with the separation Reynolds number. The plateau pressure upstream of jets and forward facing steps are very nearly identical. The ratio of plateau to free stream pressure decreases as the separation Reynolds number rises and approaches a value of approximately 2.4 at a separation Reynolds number of 2.5×10^6 for a

Mach 2.5 stream. It is evident that assuming the plateau pressure to be independent of Reynolds number, as done by Spaid and Zukoski,[3] is accurate at sufficiently high Reynolds numbers. Both the jet interaction data and the forward facing step data support the conclusion that the "free interaction" model[16] relates the wall pressures in the separated flow regions upstream of various obstacles, and that the plateau pressure is correlated by the separation Reynolds number when the free stream Mach number is constant.

The separation distance and wall pressure level vary simultaneously with Reynolds number in such a way (Fig. 8) that the amplification factor is almost independent of the Reynolds number, as seen in Fig. 10. The results for nitrogen and helium injection are very similar, and indicate a very slight increase in amplification factor with Reynolds number. However, the increase seen in Fig. 10 is not experimentally significant. This result agrees very well with results reported by Werle[8] indicating no change in amplification factor through a limited Reynolds number range. Other data are not available for comparison. It is therefore concluded that the amplification factor is insensitive to free stream Reynolds number changes.

Effect of Injectant Specific Heat Ratio

A few wind tunnel runs were made to examine the effect of changing the injectant specific heat ratio, γ_j. The effect of γ_j variation was studied by injecting hydrogen ($\gamma_j = 1.4$) and helium ($\gamma_j = 1.67$) at conditions for which the other important parameters could be matched. Wall pressure distributions typical of this experiment are seen in Fig. 11. The difference between these two curves is very small, and is due to a slight mismatch in the density, or R_jT_{oj}/R_aT_a, ratio. The amplification factor for these two cases differs insignificantly. The semi-empirical analyses of Spaid and Zukoski,[3] and recently of Werle et al.[4] predict an amplification factor increase of approximately twenty percent when γ_j increases from 1.4 to 1.67. The results of this investigation demonstrate that the separation distance, plateau pressure, and amplification factor do not increase with the injectant specific heat ratio. Although not generally recognized, this result was previously demonstrated by Allan,[15] who maintained a nominally constant R_jT_{oj}/R_aT_a by injecting nitrogen ($\gamma_j = 1.4$, $R_j = 28$) and ethane ($\gamma_j = 1.22$, $R_j = 30.1$) in a cold flow experiment. The increase in separation distance and amplification factor observed when helium was substituted for nitrogen as an injectant[3] was due to the change in R_jT_{oj}/R_aT_a, rather than the specific heat ratio change to which it was attributed. On the basis of this work and that of Allan,[15] it is concluded that the separation distance, plateau pressure, and amplification factor are insensitive to changes in the injectant specific heat ratio.

Effect of Free Stream Specific Heat Ratio

A check into the importance of the free stream specific heat ratio, γ_f, was made. It was suspected that, since γ_f depends on temperature, variations in this parameter might be important for the range of temperatures investigated. To determine the magnitude of this effect, the free stream temperature was doubled (γ_f changed from 1.40 to 1.32) and the other parameters were adjusted to duplicate the Reynolds number pressure ratio, and the ratio $R_j T_{oj}/R_a T_a$. Flowfield changes due to variation seem to be small, but measurable. The plateau pressure increases slightly (approximately 2%) as γ_f decreases from 1.40 to 1.32, but the separation distance remains approximately constant. It is apparent that changes in the free stream specific heat ratio have only a slight effect on the upstream separated flow region.

Transport Phenomena

Recirculation region composition. - Gas samples were withdrawn from the recirculation region through the pressure taps during the flowfield investigation. The taps were usually unmodified, but small probes were bonded into the pressure taps during several wind tunnel runs. These measurements demonstrate that the axial distribution of injectant in the recirculation region is similar to the wall pressure distribution. There are "concentration plateaus," much like the pressure plateau. The wall pressure approaches the plateau pressure level a short distance downstream of the separation point. The concentration plateau is approached in a similar manner, but the distance from the separation point to the start of the concentration plateau is approximately twice the corresponding distance associated with the pressure rise. This region of nearly uniform composition encompasses the major portion of large recirculation regions. The fraction of injectant in this region is high, a mole fraction near forty percent being typical for hydrogen injection. As is shown in this section, the gas sampling measurements imply substantial mass flow rates of injectant and air into and out of the recirculation region.

The composition of the recirculation region was insensitive to variation of any parameter except the ratio $R_j T_{oj}/R_a T_a$. Injectant distributions in the recirculation region typical of two values of this parameter are presented in Fig. 12. $R_j T_{oj}/R_a T_a$ was changed by varying the injectant temperature in this helium injection example. Identical dependence on this parameter was found when the injectant or the free stream temperature was varied. The mass fraction of injectant at the concentration plateau, Y_p, was correlated with $R_j T_{oj}/R_a T_a$ for all of the wind tunnel runs made during this investigation, as seen in Fig. 13. Variation of the jet to free stream pressure ratio, p_{oj}/p_f, from 40 to 110 had no discernible effect on the distribution of nitrogen, helium, or hydrogen injectant in the separated flow region, if $R_j T_{oj}/R_a T_a$ was held constant. Increasing the free stream unit Reynolds number by a factor of six did not change the plateau concentration. The plateau mass fractions measured throughout the range of conditions of this investigation are plotted in Fig. 13. The recirculation region plateau mass fraction is very well correlated by the relation

$$Y_p = 0.23\left(\frac{R_j T_{oj}}{R_a T_a}\right)^{-1/2}$$

This curve is drawn through the data in Fig. 13. It is evident that the recirculation region composition depends strongly upon the ratio, $R_j T_{oj}/R_a T_a$, and seems to be independent of the other parameters investigated. Comparison of this result with previous gas sampling measurements in this region is not possible. To the author's knowledge, such measurements have not previously been made.

Mass Transport Rates

The ratio of the injectant and air transport rates through the recirculation region can be calculated from composition measurements using Eq. (3). The existence of a large, almost homogeneous, portion of the recirculation region lends substantial support to the "well mixed" assumption on which Eq. (3) is based. A tracer gas injection experiment, also based on this assumption, was carried out to determine the mass flux of air across the separated turbulent boundary layer. The results of this experiment and the recirculation region composition measurements make possible estimates of the air and injectant mass transport rates through the recirculation region.

Helium tracer gas was injected into the recirculation region upstream of forward facing steps. These experiments were conducted through a range similar to that covered in the transverse injection investigation. The tracer gas was metered and injected from ten small tubes evenly spaced across the model just upstream of the step. Gas sampling and wall pressure measurements were made as in the jet interaction experiments. This data was used in Eq. (5) and (7) to evaluate the dimensionless transport mass flux through the separated boundary layer, W_{ar}. Within the accuracy of this investigation, this quantity remained constant and equal to 0.023. This result was used in Eq. (8), with the flowfield properties measured in the jet interaction experiments, to evaluate the injectant mass transport rate into the recirculation region. The estimated injectant transport rates are plotted in Fig. 14 as the fraction of the total injectant mass flow rate, $\dot{m}_j$. The data presented in Fig. 14 represent the entire range of conditions examined during this investigation. Approximately five percent of the gas injected passes through the recirculation region. This fraction seems to decrease as the ratio of the air to injectant temperature increases. The same data may be used in Eq. (9) to evaluate the residence time of gases in the recirculation region. A typical residence time is approximately 0.5 msec.

V. Conclusions

The effects of independent variation of p_{oj}/p_f, R_jT_{oj}/R_aT_a, γ_j, γ_f, and the free stream Reynolds number have been determined. The separation distance, plateau pressure, and amplification factor were significantly affected by changes in p_{oj}/p_f and R_jT_{oj}/R_aT_a. Only small changes resulted from varying the free stream Reynolds number. The jet to free stream pressure ratio has a very strong effect on the size of the upstream separated flow region. The dependence of the separation distance on p_{oj}/p_f is correlated by

$$\frac{x_{sep}}{d_s} = a\left(\frac{p_{oj}}{p_f}\right)^{0.77}$$

throughout the range covered in this experiment. The coefficient, a, is a function of both the separation Reynolds number and the ratio R_jT_{oj}/R_aT_a. The free stream Reynolds number affects the separation distance and the wall pressure in the separated flow region. Through the Reynolds number range of this experimental program, the ratio of plateau to free stream pressure decreases as the Reynolds number increases, asymptotically approaching a value of approximately 2.4 at very high separation Reynolds numbers. While the plateau pressure decreases, the separation distance increases with the Reynolds number. The net effect of a Reynolds number change on the interaction force and the amplification factor is very small. The jet temperature and molecular weight strongly influence the separation distance when low molecular weight or high temperature gases are injected. This effect is correlated by the ratio R_jT_{oj}/R_aT_a. Two regimes of dependence on this parameter are found. At values of R_jT_{oj}/R_aT_a below 7, the separation distance is not affected by changes in this parameter. As R_jT_{oj}/R_aT_a is increased above 7, the separation distance rapidly increases, causing a similar increase in side force and amplification factor. Changes in γ_j and γ_f have little effect on the flowfield. Existing semi-empirical methods for calculating the jet interaction flowfield will have to be extensively modified to be consistent with these results.

Gas sampling measurements in the upstream recirculation region have demonstrated that this region has a high injectant concentration at all conditions investigated. A concentration plateau, similar to the wall pressure plateau, occurs in the separated flow region. The mass fraction of injectant at the concentration plateau is correlated by the relation

$$Y_{plat} = 0.23\left(\frac{R_jT_{oj}}{R_aT_a}\right)^{-1/2}$$

The fact that a large portion of the recirculation region has this uniform, plateau concentration substantially verifies the "well mixed" flow model. The dimensionless transport mass flux across the separated boundary layer, $W_{ar} = \dot{m}/x_{ss}s\rho_f u_f$, does not depend on the free stream temperature, Reynolds number, and the separated region size, and is approximately equal to 0.023. Approximately five percent of the mass injected from the slot nozzle passes through the upstream recirculation region. Within experimental accuracy, this fraction is independent of the species injected. These transport measurements, the inert flow geometry measurements, and an equation developed from the "well mixed" flow model have been used to show that the residence time of reactants in this region is long.

References

1. Sterrett, J. R. and Barber, J. B., "A Theoretical and Experimental Investigation of Secondary Jets in a Mach 6 Free Stream with Emphasis on the Structure of the Jet and Separation Ahead of the Jet," TM X-57137, 1966, NASA, Langley Station, Va.

2. Hawk, N. E., and Amick, J. L., "Two-Dimensional Secondary Jet Interaction with a Supersonic Stream," AIAA Journal, Vol. 5, No. 4, April 1967, pp. 655-660.

3. Spaid, F. W., and Zukoski, E. E., "A Study of the Interaction of Gaseous Jets from Transverse Slots with Supersonic External Flow," AIAA Journal, Vol. 6, No. 2, February 1968, pp. 205-212.

4. Werle, M. J., Driftmyer, R. T., and Shaffer, D. G., "Jet-Interaction-Induced Separation of Supersonic Turbulent Boundary Layers - The Two Dimensional Problem," Paper No. 70-765, June-July 1970, AIAA, Los Angeles, Calif.

5. Thayer, W. J., III, and Corlett, R. C., "Ignition and Combustion of a Transverse Hydrogen Jet in a Mach 2.5 Airstream," Paper WS/CI-71-15, Western States Section/The Combustion Institute, Denver, Colorado, April 1971.

6. Longwell, J. P., Frost, E. E., and Weiss, M. A., "Flame Stability in Bluff Body Recirculation Zones," Industrial and Engineering Chemistry, Vol. 45, No. 8, August 1953, pp. 1629-1633.

7. Longwell, J. P. and Weiss, M. A., "High Temperature Reaction Rates in Hydrocarbon Combustion," Industrial and Engineering Chemistry, Vol. 47, No. 8, August 1955, pp. 1634-1643.

8. Werle, M. J., "A Critical Review of Analytical Methods for Estimating Control Forces Produced by Secondary Injection: The Two Dimensional Problem," NOLTR-68-5, January 1968, Naval Ordnance Laboratory, White Oak, Maryland.

9. Shreeve, R. P. and Richmond, J. K., "Design and Operation of the BSRL Pebble Bed Heater - Windtunnel Facility," D1-82-0577, October 1966, Boeing Scientific Research Laboratories, Seattle, Washington.

10. Thayer, W. J., III, "The Two-Dimensional Separated Flow Region Upstream of Inert and Chemically Reactive Transverse Jets," Ph.D. Thesis, 1971, University of Washington; also D1-82-1066, March 1971, Boeing Scientific Research Laboratories, Seattle, Washington.

11. Werle, M. J., Driftmyer, R. T., and Shaffer, D. G., "Two-Dimensional Interaction Experiments Results of Flowfield and Scale Effect Studies," Proceedings of the 8th Navy Symposium on Aeroballistics, Naval Ordnance Lab., Vol. 3, 1969, pp. 865-884.

12. Thayer, W. J., III, "New Information on the Two-Dimensional Jet Interaction Problem," AIAA Journal, Vol. 9, No. 3, March 1971, pp. 539-541.

13. Crist, S., Sherman, P. M., and Glass, D. R., "Study of the Highly Underexpanded Sonic Jet," AIAA Journal, Vol. 4, No. 1, January 1966, pp. 68-71.

14. Spaid, F. W., "A Study of Secondary Injection of Gases into a Supersonic Flow," Ph.D. Thesis, June 1964, California Institute of Technology.

15. Allan, W. L., "An Experimental Investigation of the Aerodynamic Force Characteristics of a Jet Issuing Transverse to a Wedge, Final Report," CR-96722, January 1968, NASA.

16. Chapman, D. R., Kuehn, D. M., and Larson, H. K., "Investigation of Separated Flows in Supersonic and Subsonic Streams with Emphasis on the Effect of Transition," TN 3869, March 1957, NACA, Moffett Field, Calif.

17. Love, E. S., "Pressure Rise Associated with Shock-Induced Boundary-Layer Separation," TN 3601, December 1955, NACA, Langley Field,

18. Hahn, J. S., "Experimental Investigation of Turbulent Step-Induced Boundary-Layer Separation at Mach Numbers 2.5, 3, and 4," AEDC-TR-69-1, March 1969, ARO, Incorporated, Arnold Air Force Station, Tennessee.

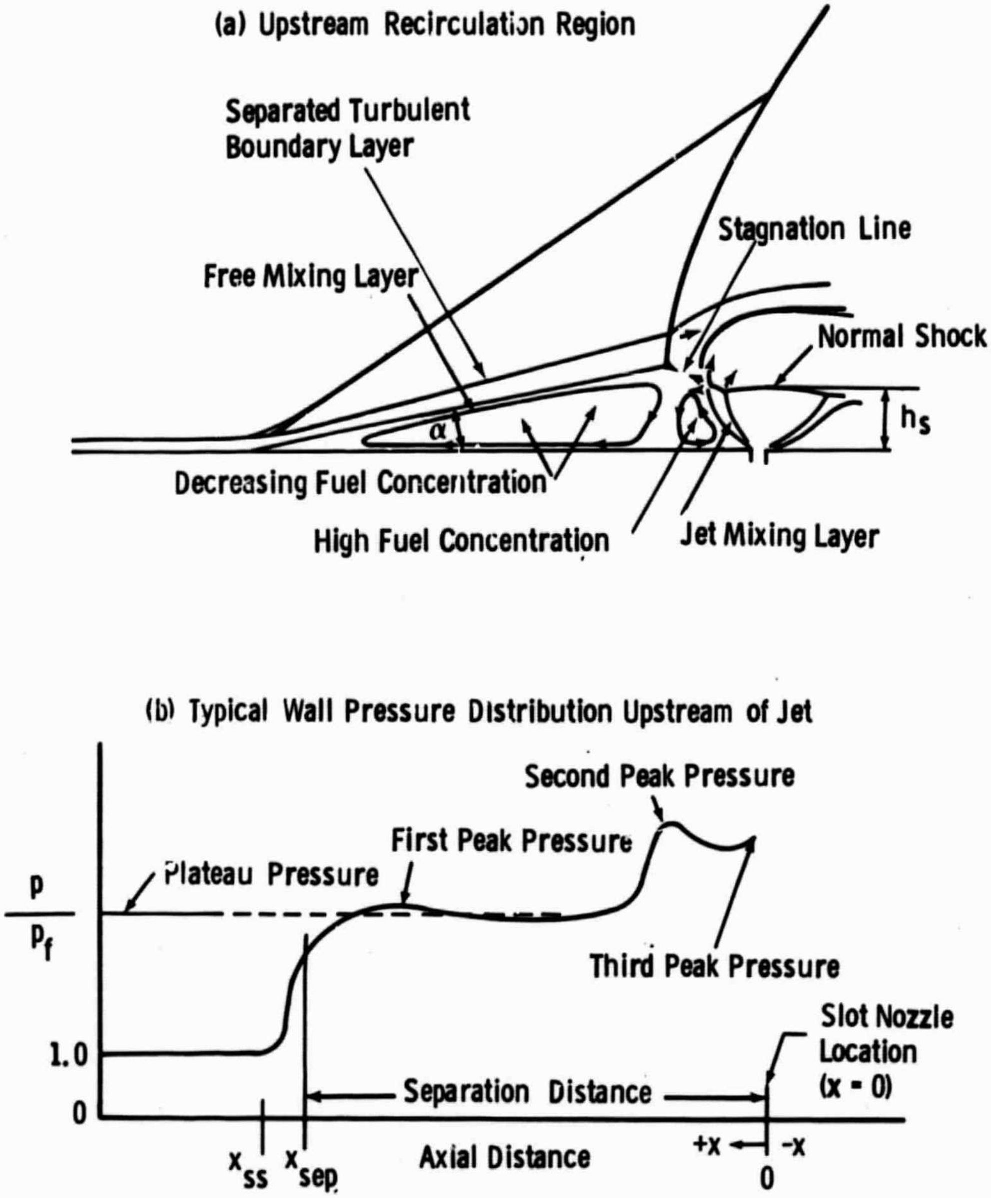

Figure 1. - Upstream recirculation region of the jet interaction flowfield.

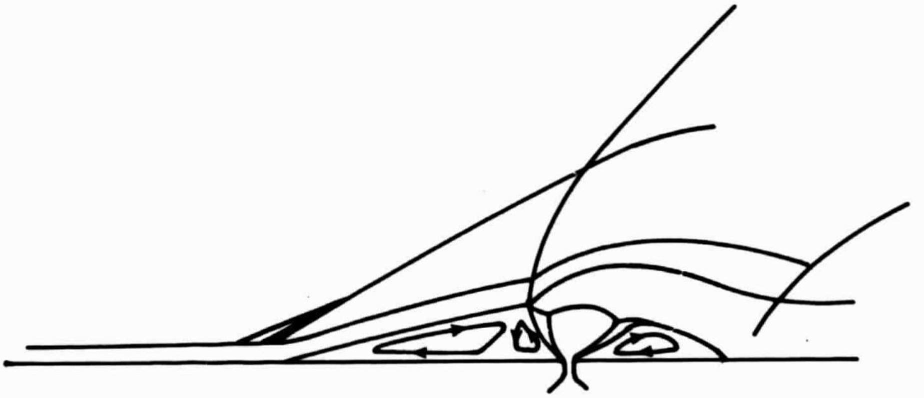

a) Jet Interaction Flowfield

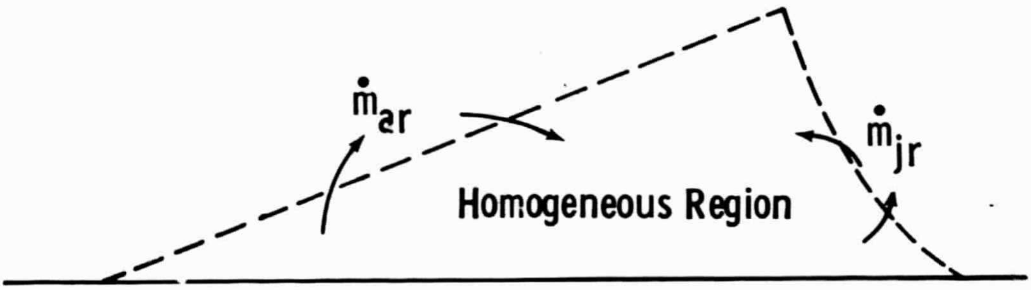

b) Idealized Recirulation Region

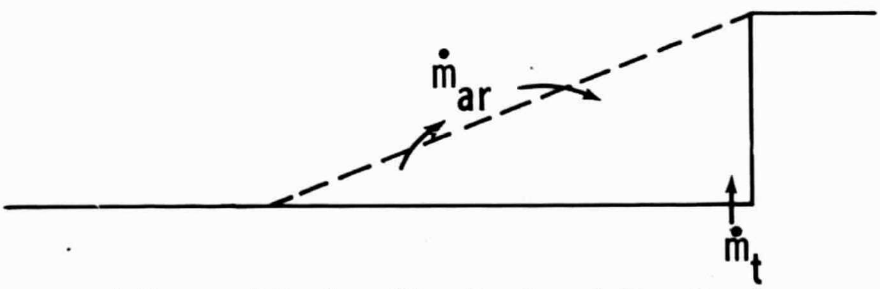

c) Forward Facing Step Recirculation Region

Figure 2. - Control volumes used for transport considerations.

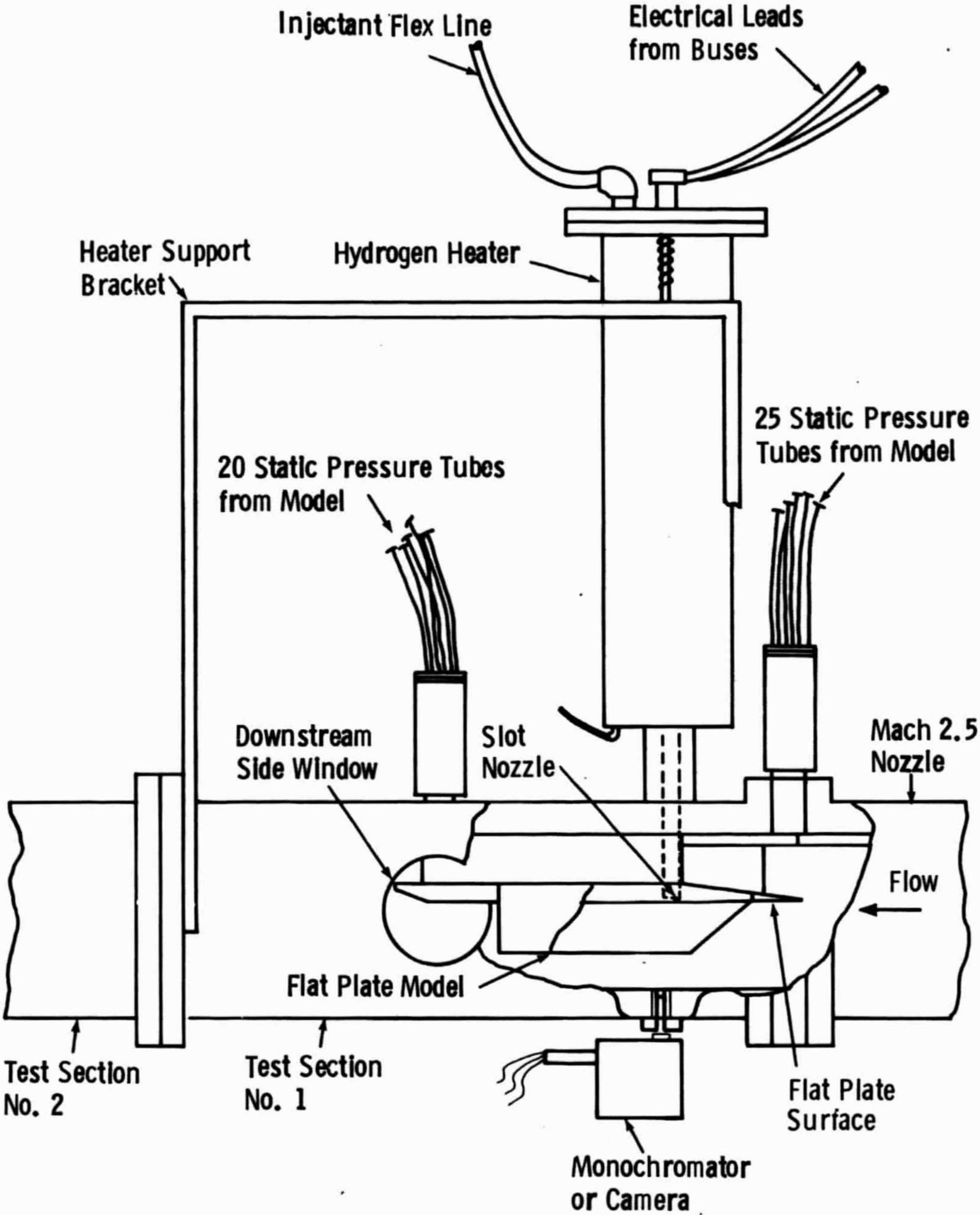

Figure 3. - Flat plate model installed in the wind tunnel.

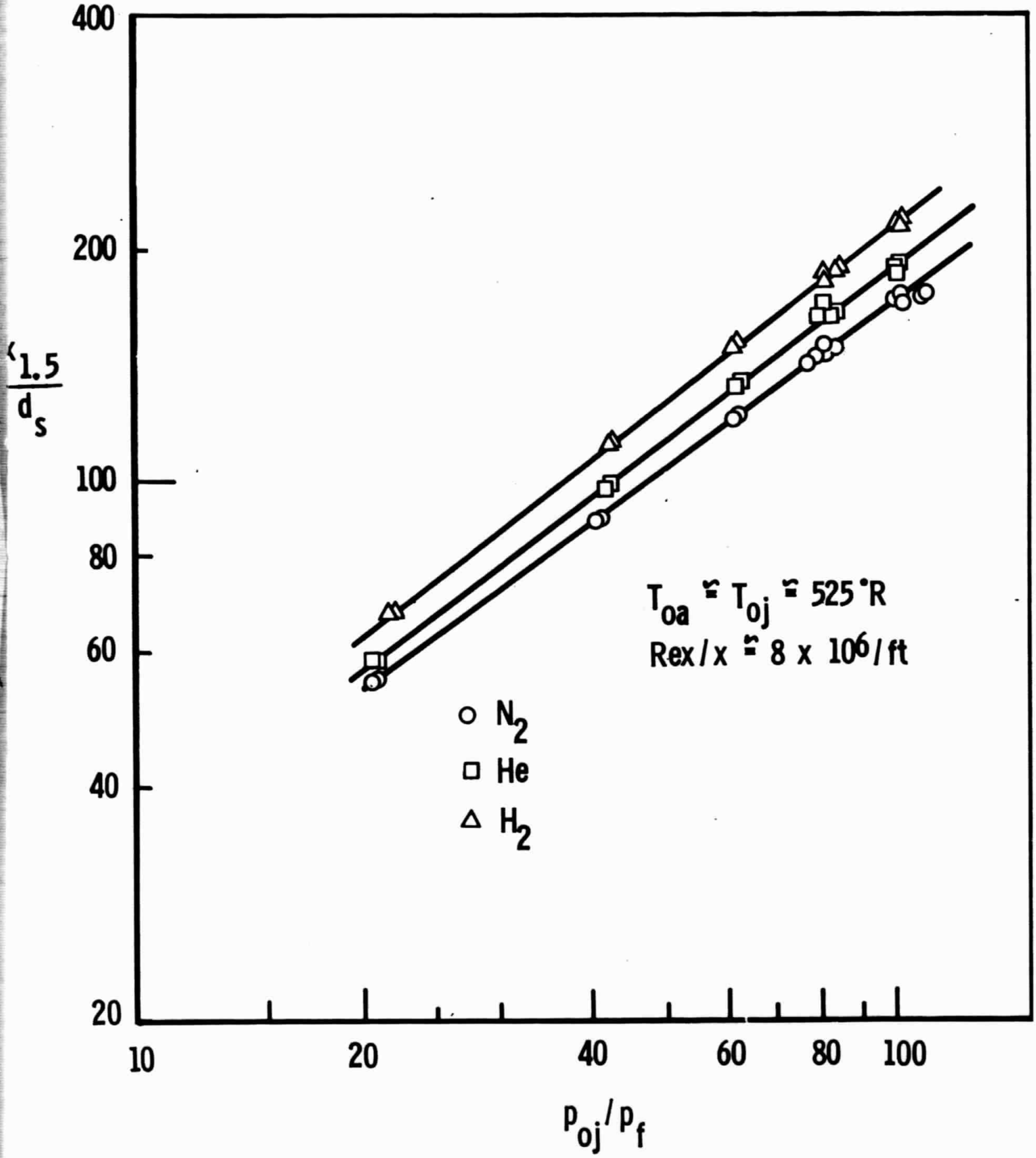

Figure 4. - Correlation of separation distance dependence on the jet to free stream pressure ratio.

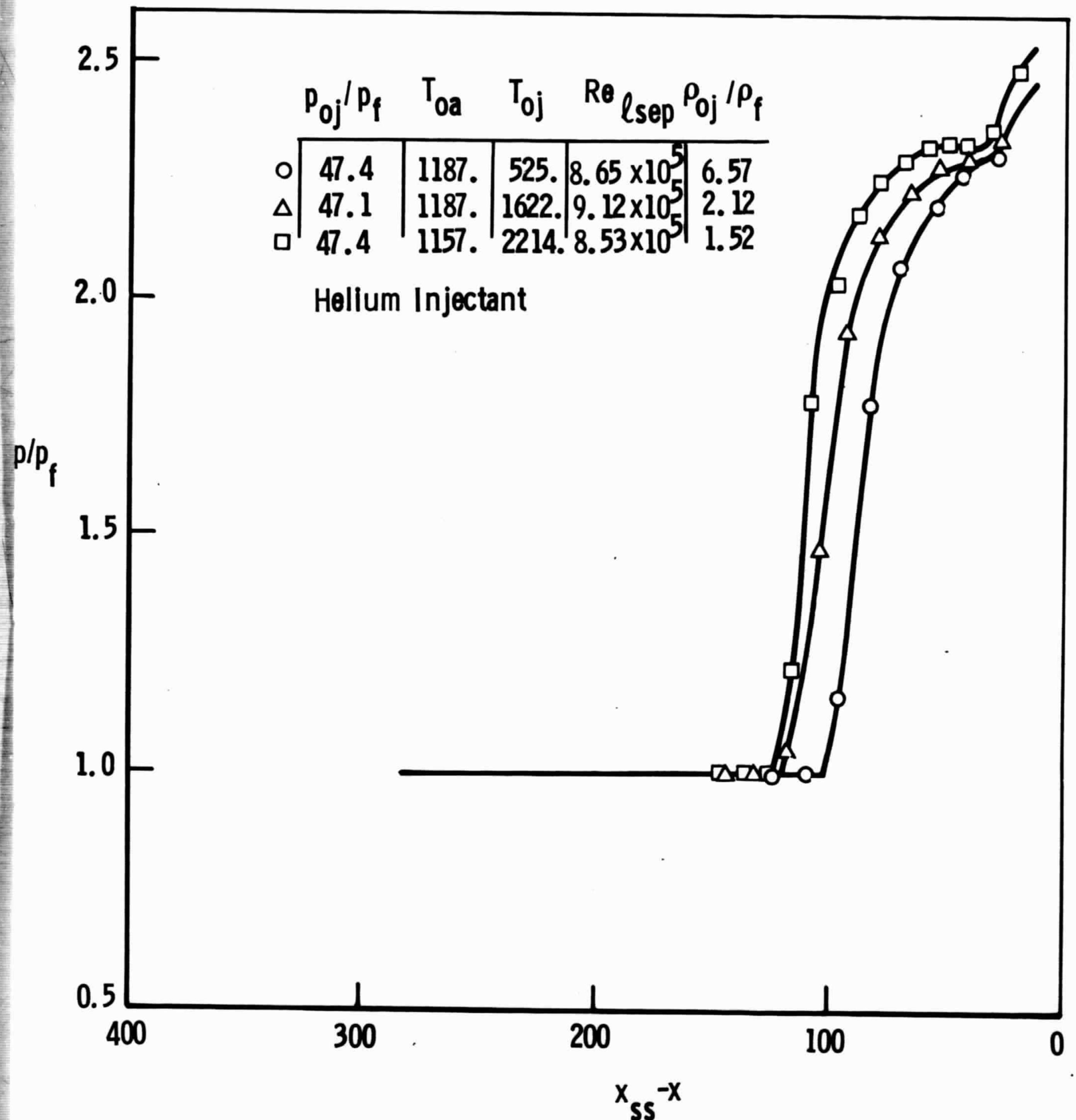

Figure 5. - Comparison of wall pressures at several values of the density

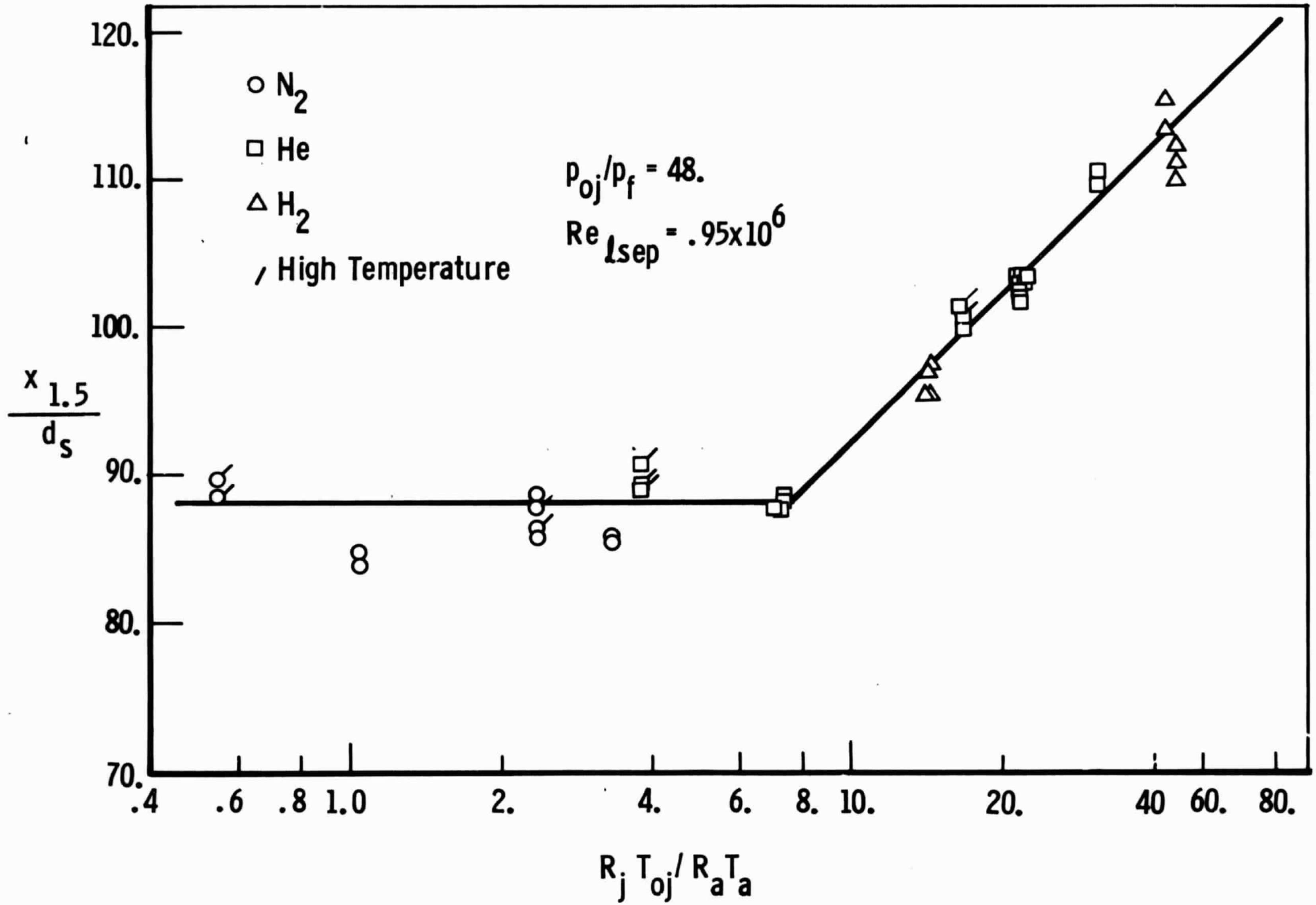

Figure 6. - Dependence of the separation distance on temperature and molecular weight.

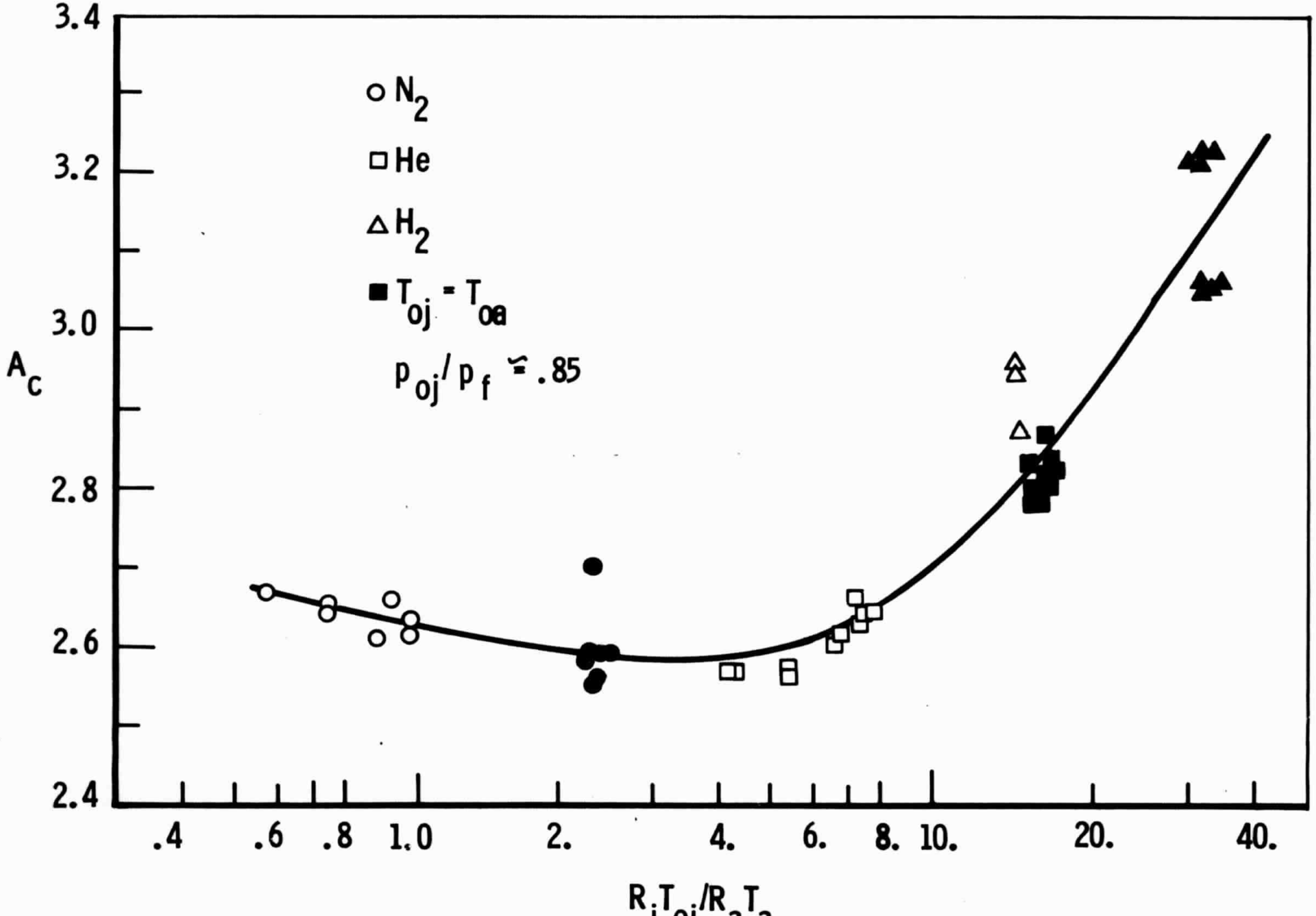

3.4
3.2
3.0
2.8
2.6
2.4
A_c
○ N_2
□ He
△ H_2
■ T_oj = T_oa
p_oj/p_f ≅ .85
.4
.6
.8
1.0
2.
4.
6.
8.
10.
20.
40.
R_j T_oj/R_a T_a

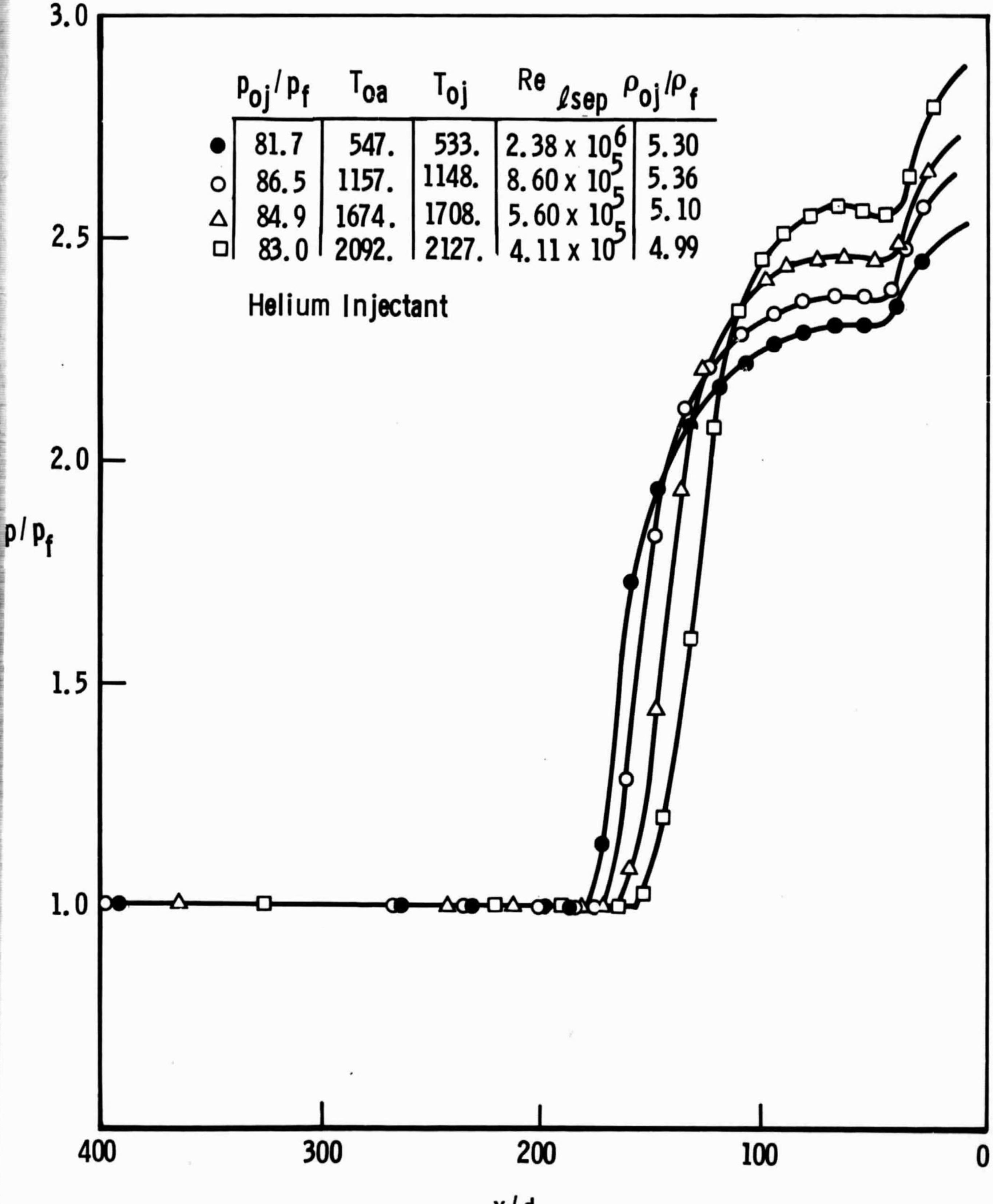

Figure 8. - Comparison of wall pressure at several values of $Re_{\ell sep}$ for helium jets with $T_{oa} = T_{oj}$.

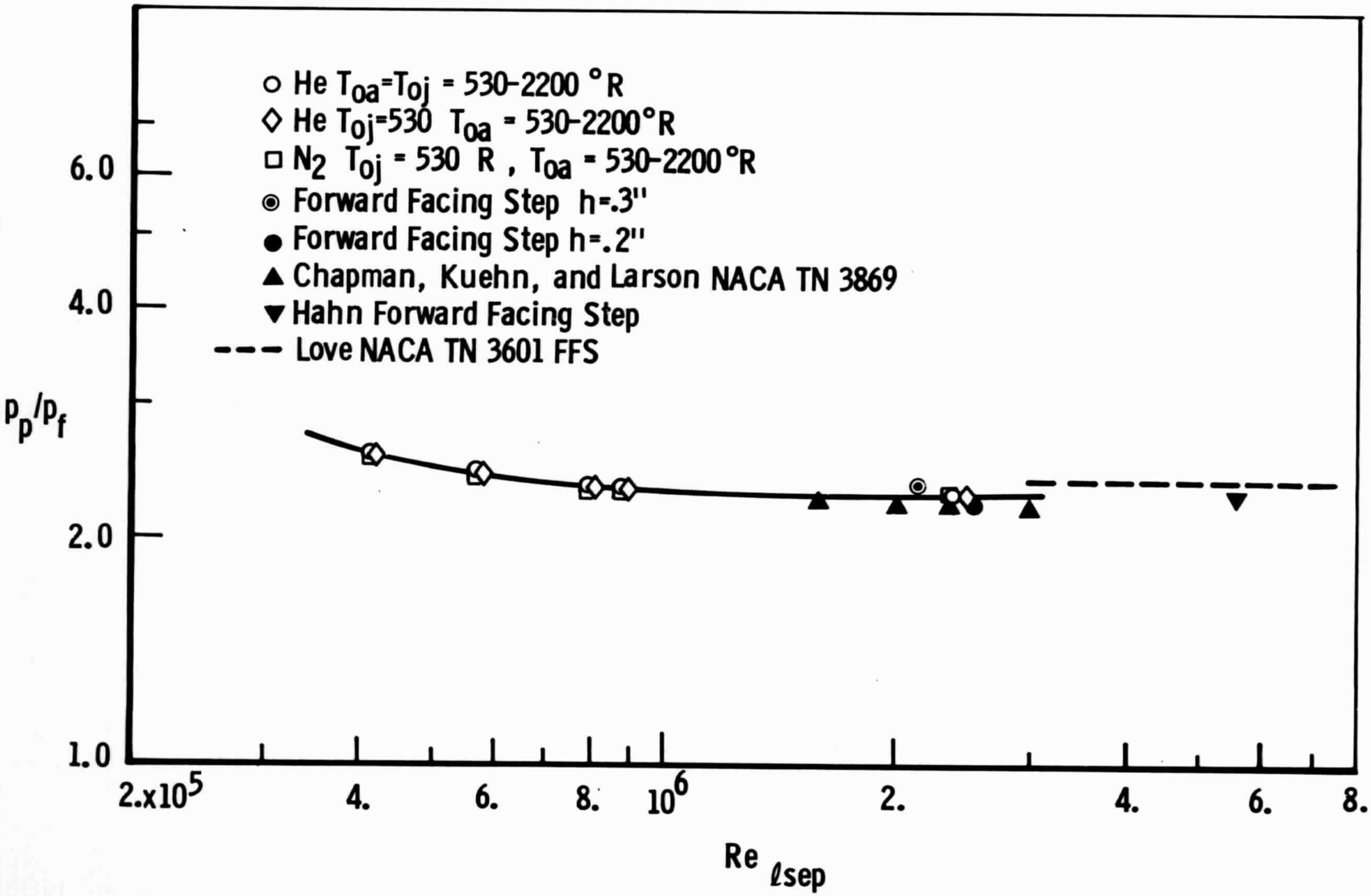

Figure 9. - Dependence of separation region plateau pressure on the separation Reynolds number.

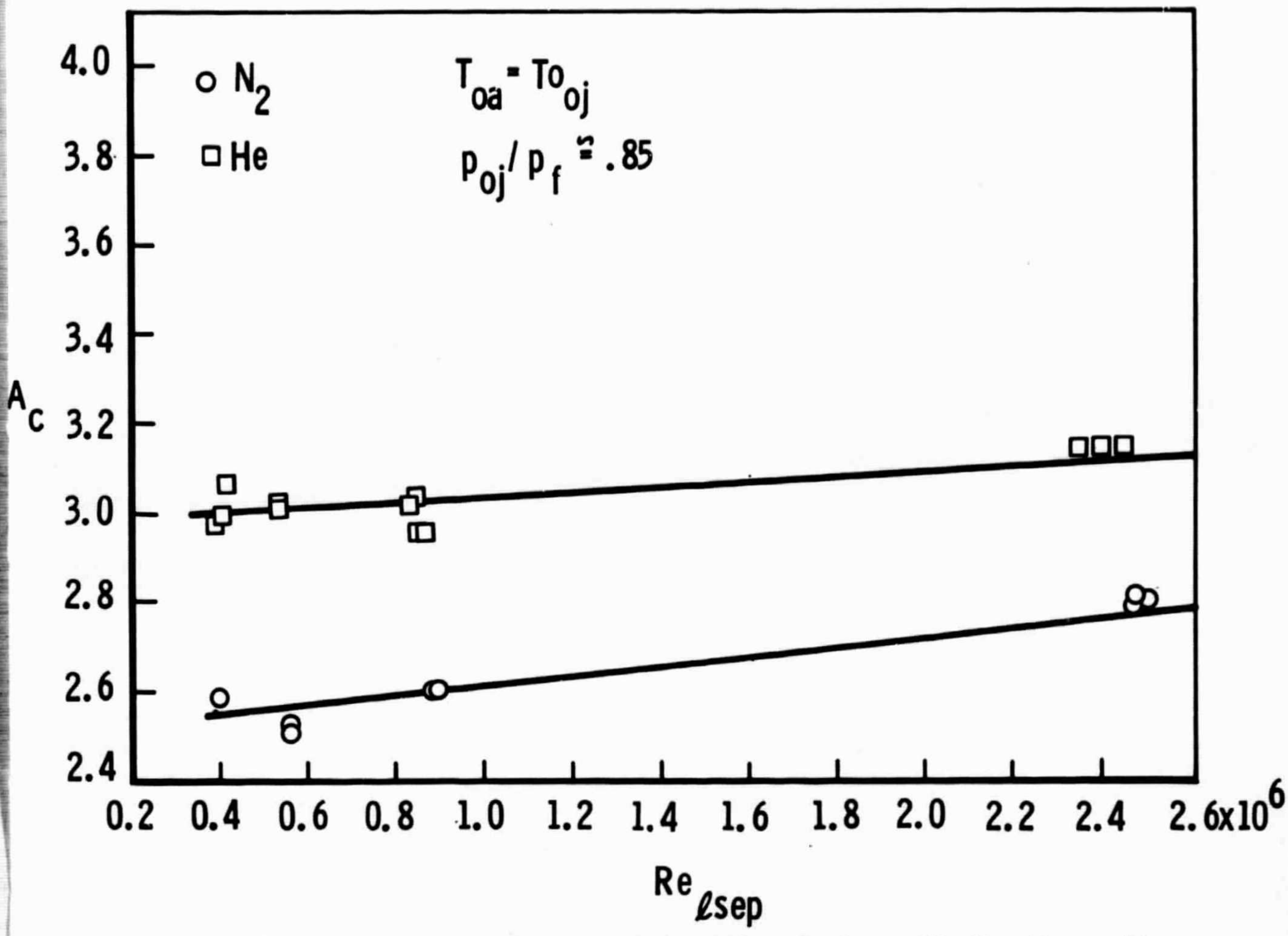

Figure 10. - Variation of the amplification factor with the Reynolds number at separation.

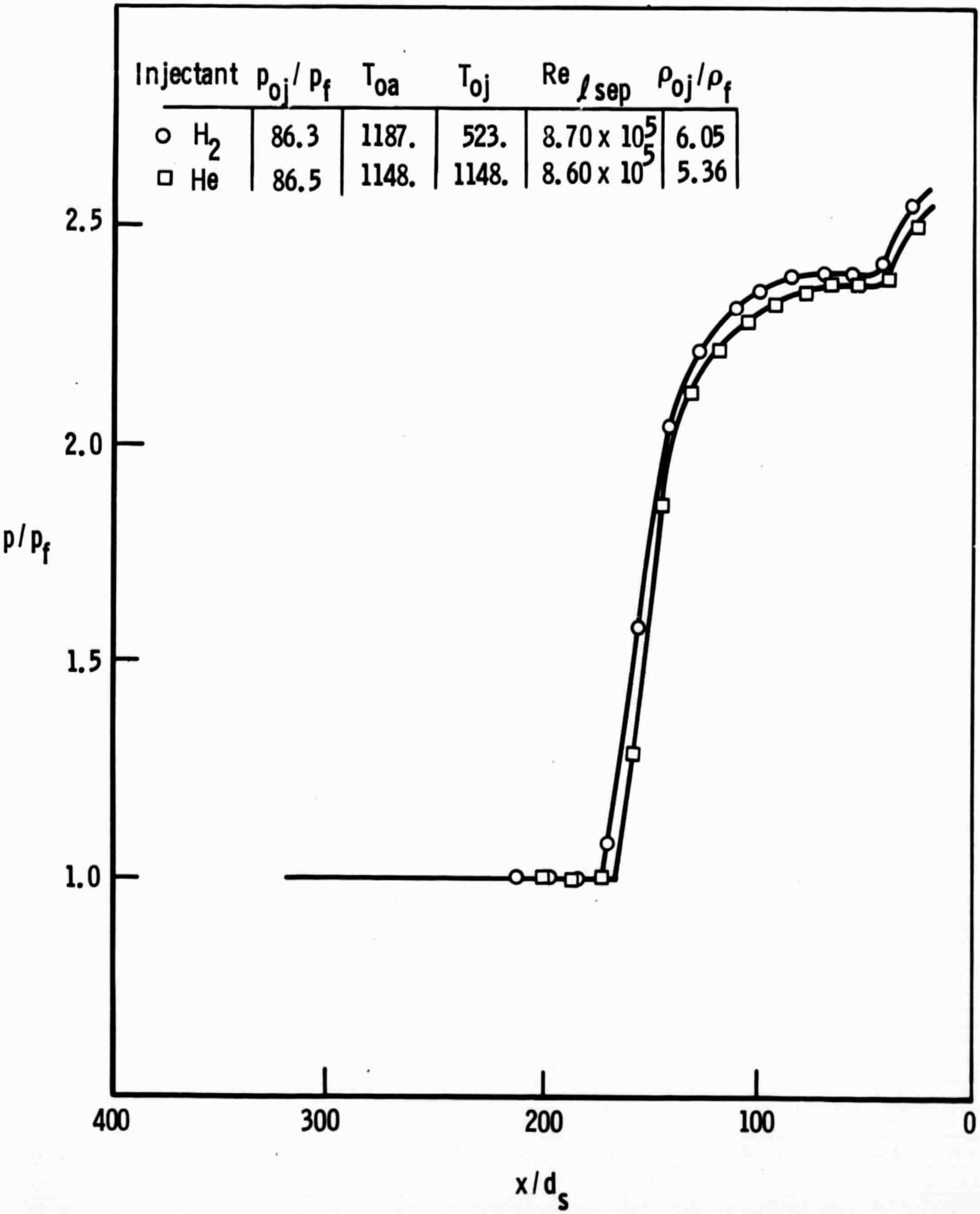

Figure 11. - Comparison of wall pressures for hydrogen and helium injection at constant density ratio.

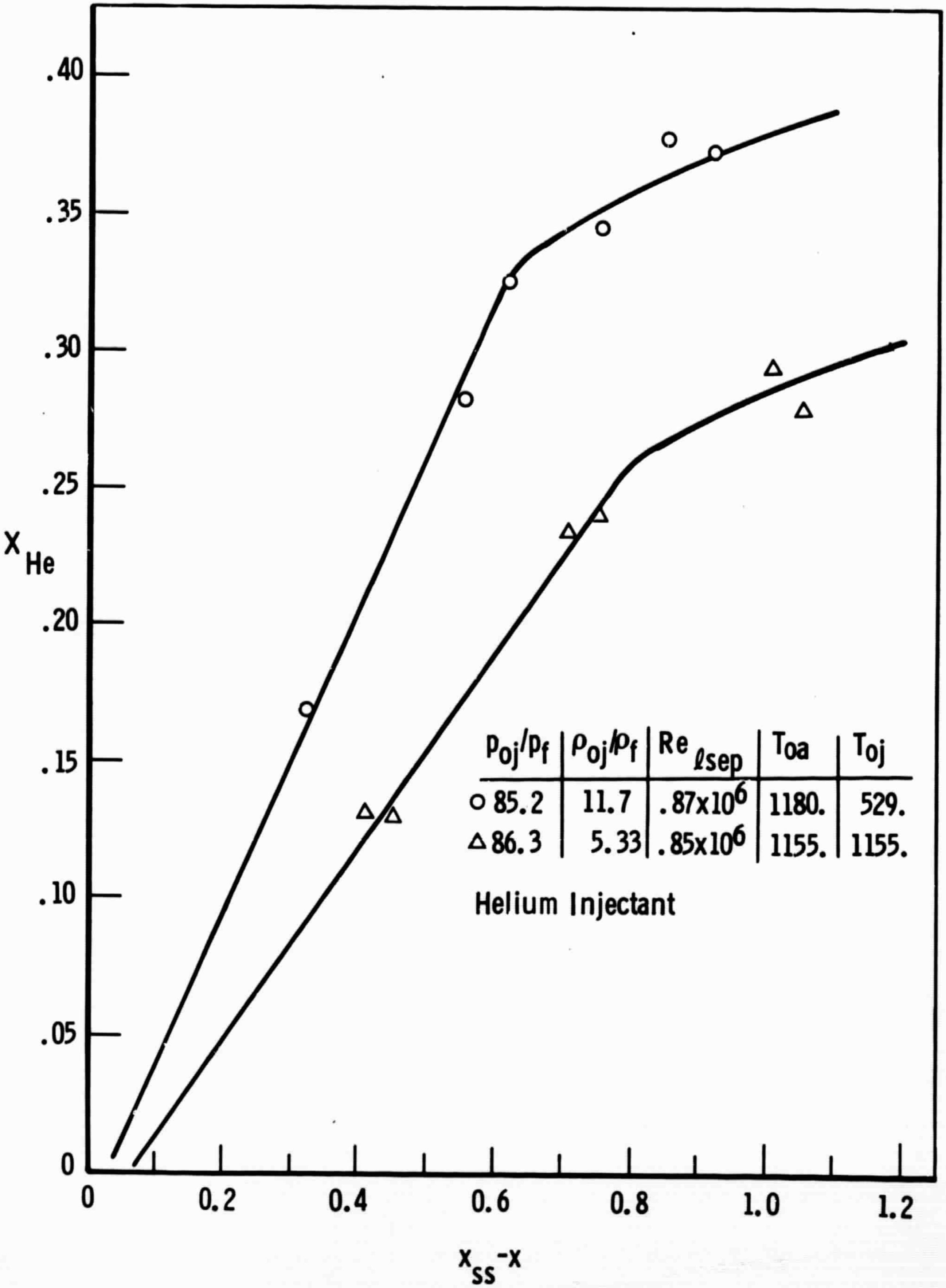

Figure 12. - Comparison of recirculation region injectant concentration at two values of the density ratio.

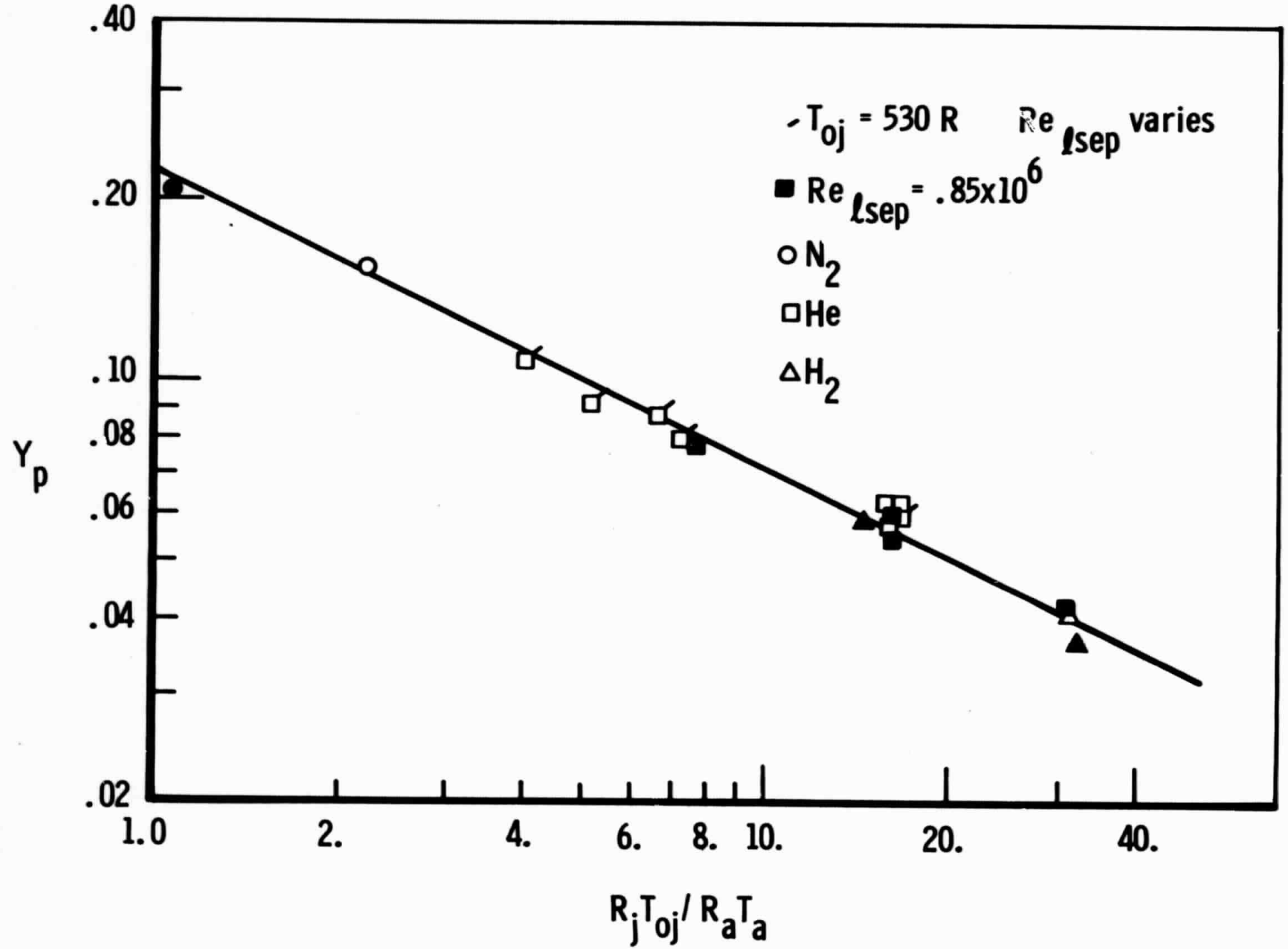

Figure 13. - Correlation of the plateau mass fraction with the ratio R_jT_{oj}/R_aT_a.

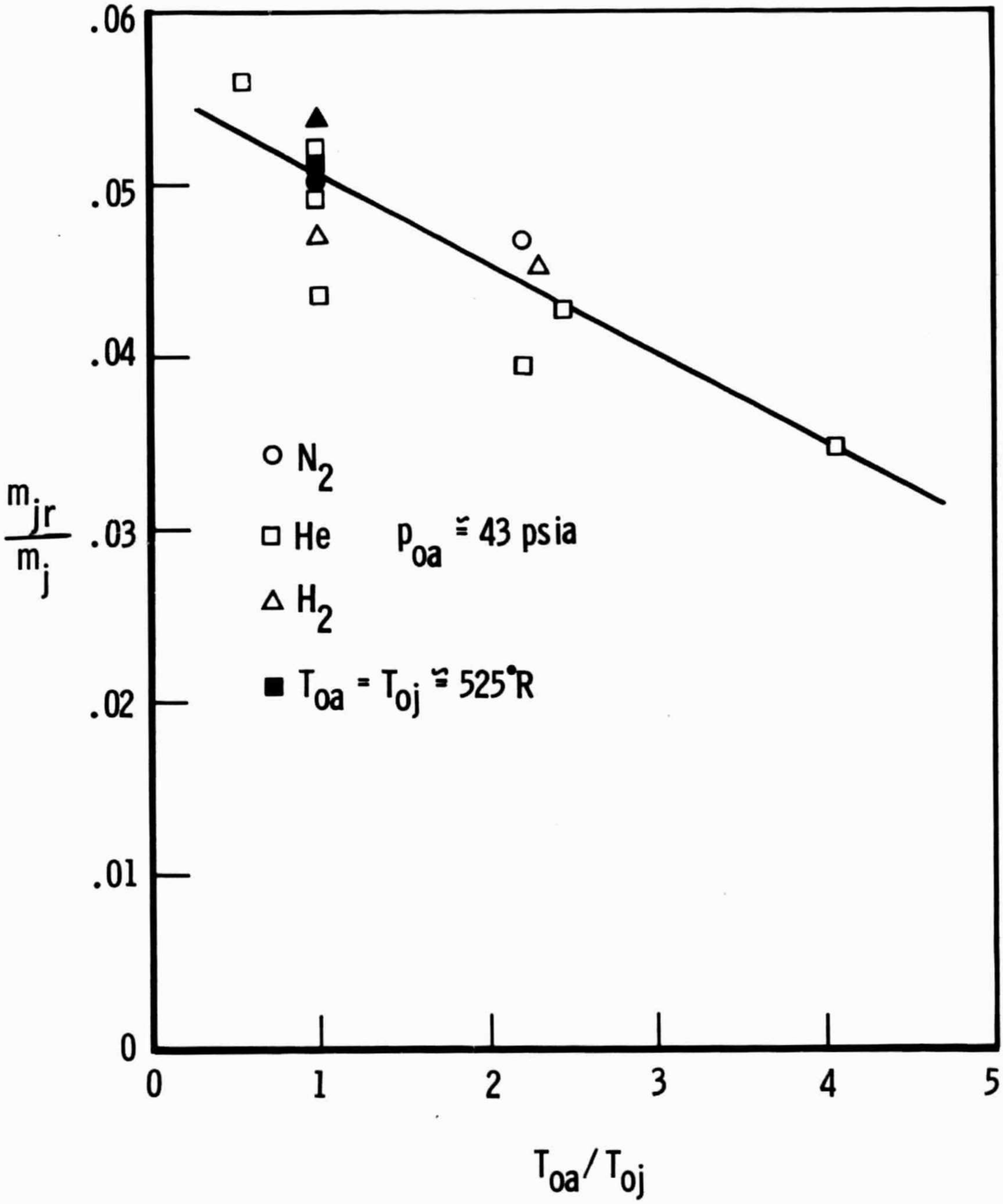

Figure 14. - Estimated injectant mass flow rates through the upstream recirculation region.